Available online at www.sciencedirect.com
ScienceDirect
ELSEVIER
Vision Research 47 (2007) 818–827
Vision Research
www.elsevier.com/locate/visres

Closure facilitates contour integration

Birgit Mathes [a,*], Manfred Fahle [a,b]

[a] *University of Bremen, Department of Human Neurobiology, Argonnenstr. 3, 28211 Bremen, Germany*
[b] *The Henry Wellcome Applied Vision Research Centre, Tait Building, Northampton Square, London EC1V OHB, UK*

Received 29 June 2006; received in revised form 18 October 2006

Abstract

Closed contours are often better perceived than those not fully enclosing an area, i.e., open contours. This facilitation of contour integration by closure, however, has been questioned arguing that in earlier studies closed contours were often "smoother" than open ones, because open contours usually had turning points. To solve this controversy, we compared detection performance for closed circles or ellipses of a *higher* curvature with open contours of a *lower* curvature neither having any turning points. Performance for circles and ellipses declined with increasing gap size and recovered only for contours with very low curvatures. Furthermore, performance increased with increasing number of contour elements and was better for smooth compared to S-shaped contours that change direction of curvature. Our results clearly demonstrate that closure improves contour detection, even though this advantage might be minor. The advantage of closed contours is maximal compared to open contours of similar curvature.

Keywords: Contour integration; Closure; Curvature; Orientation; Circularity; Number of contour elements

1. Introduction

The detection of objects requires the perceptual organisation of a visual scene to separate the object from its background as described by Gestalt grouping principles (Westheimer, 1999; Wertheimer, 1923). In this study, we investigated whether closure facilitates the Gestalt principle of good continuation using the contour integration paradigm. Two additional factors investigated were "smoothness", i.e., the occurrence versus absence of turning points, and the number of contour elements constituting a target. In our task, the contour is hidden in a surround of randomly oriented elements (Field, Hayes, & Hess, 1993; Hess & Field, 1999). The detection of a discontinuous contour is based on the spatial integration of oriented elements aligned with this contour and the separation of the contour from its surround (see Fig. 1).

It has been repeatedly demonstrated by varying the ratio between contour and background element densities that spatial integration of contour elements is more effective for closed than for open contours (Kovacs & Julesz, 1993; Pettet, McKee, & Grzywacz, 1998), even though the effect might be small (Braun, 1999) and restricted to closed contours without sharp edges (Kovacs & Julesz, 1993; Pettet et al., 1998). At least for certain element-to-element distances, detection of closed contours also show an advantage over open contours when element density is kept comparable between contour and background elements (Beaudot & Mullen, 2003). Although this effect has not been found in all studies (Tversky, Geisler, & Perry, 2004), closed contours seem to allow a larger orientation jitter, i.e., a larger deviation of the orientations of contour elements from the optimally alignment, than open contours do (see Fig. 1, Mathes & Fahle, 2007; Poom, 2002).

However, the implication that better performance for closed contours results from their closure has been challenged (Braun, 1999; Pettet, 1999; Pettet et al., 1998; Tversky et al., 2004). Studies investigating the closure-effect

* Corresponding author. Fax: +49 421 218 9525.
E-mail address: birgit.mathes@uni-bremen.de (B. Mathes).
URL: http://www.humanbio.uni-bremen.de (B. Mathes).

0042-6989/$ - see front matter
doi:10.1016/j.visres.2006.11.014

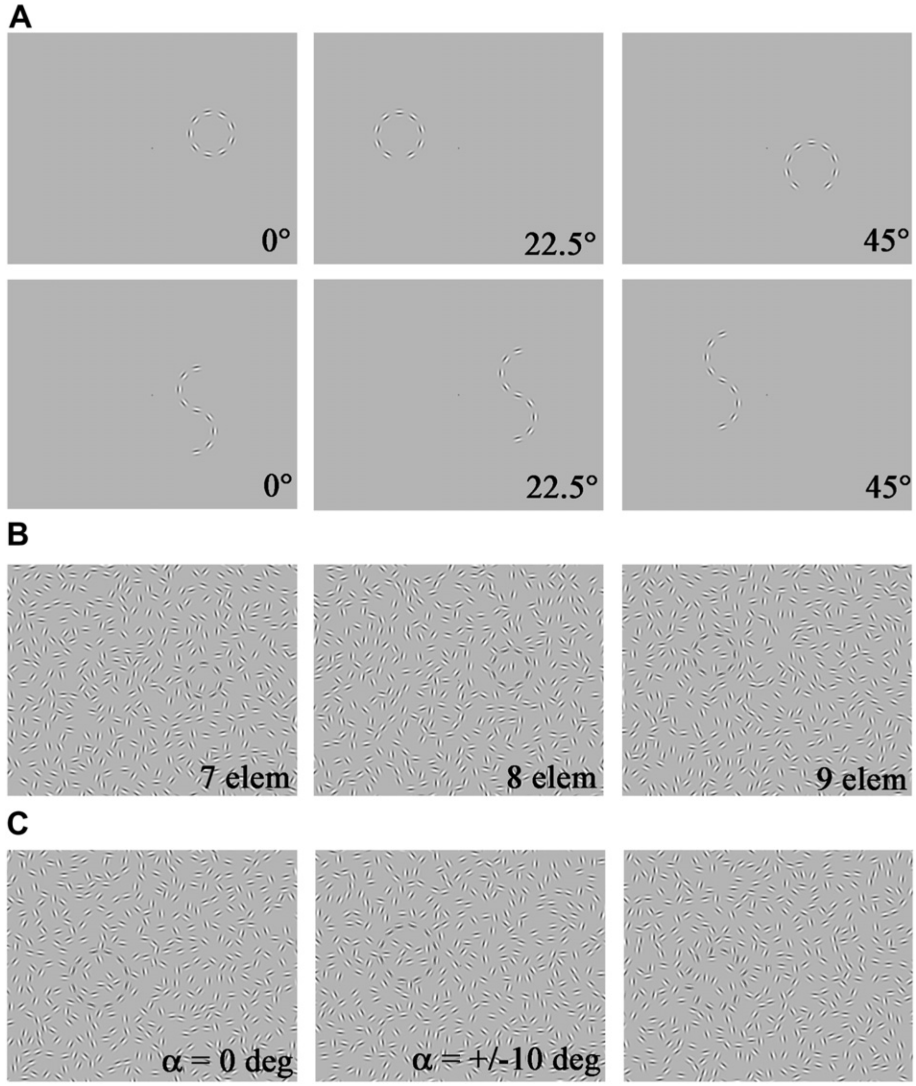

Fig. 1. (A) Illustrates the stimuli used in experiment 1. We presented closed circles (upper left corner) or open circles with either an additional gap of 22.5° or 45° (middle and right). The corresponding S-figures were created by introducing a turning point at half length. (B) In experiment 1 all contour shapes (see (A)) were tested for contours of either 7, 8 or 9 elements. After constructing the contour, the contour was embedded in a surround of pseudorandomly oriented distracters. Contours are highlighted for presentational purposes only. (C) Contour integration performance was measured by varying the orientation jitter α (in degree, Field et al., 1993). On the left side the orientation of the contour elements was set to be tangential to the closed circle ($\alpha = 0°$). Contour integration became more difficult when an orientation jitter modified the optimally aligned arrangement by rotating each contour element randomly clockwise or anticlockwise and thereby increasing α (middle). On the right side two circles are hidden. One is highlighted for presentational purposes. The second contour is undetectable since the figure and distracter element orientation are pseudo-randomised (similar but not identical to the highlighted circle). Obviously, there are no unwanted positional cues that could subserve detection of the figure.

often constructed closed contours which were easier to detect than open contours for at least one additional reason, hence possibly overestimated the influence of closure on detection performance.

Contour integration relies on many properties of the contour. An example is the average absolute angle between adjacent contour elements, i.e., the curvature of the contour (Field et al., 1993; Pettet, 1999). Therefore, most studies on contour closure controlled for the curvature of the contour (Braun, 1999; Kovacs & Julesz, 1993; Pettet et al., 1998; Poom, 2002; Tversky et al., 2004). Often open contours were constructed by "cutting up" the closed contour and "flipping" one part, i.e., by changing the sign of the angle between two adjacent contour elements at least once (Braun, 1999; Pettet et al., 1998; Poom, 2002; Tversky et al., 2004). This procedure introduced a turning point in the open contours. Unfortunately, increasing the number of turning points degrades performance even for open contours (Pettet, 1999). This finding therefore indicates that better performance for closed contours with fewer or no turning points at all might result from smoothness rather than closure.

Another strategy used to measure closure was to eliminate elements from closed contours to create open contours of fewer elements but of comparable shapes (Braun, 1999; Kovacs & Julesz, 1993). Contour integration improves with increasing number of contour elements (Braun, 1999; Li & Gilbert, 2002) but performance seems to reach a plateau for approximately 10 elements (Braun, 1999). Eliminating elements, as pointed out by Braun, is therefore only acceptable for long contours – but leads only to a minimal advantage for closure in these stimuli (Braun, 1999).

The purpose of this study was to investigate if closure facilitates contour integration even when open contours do not include additional turning points or fewer elements than closed ones. Furthermore, we controlled for comparable variability in contour shape and location between closed and open contours.

We compared contour detection for closed contours with open contours of reduced mean curvature (see Fig. 1). As mentioned above, the relation between increased performance and decreasing curvature is a robust finding in contour integration (Field et al., 1993; Pettet, 1999). Due to their lower curvature, open contours should therefore be easier to detect. But as the reduction of curvature increases gap size of open contours, the improvement through decreasing curvature might be counteracted by the loss of closure which decreases performance. Contrary, when decreasing the curvature of S-figures, which are always open, contour integration should depend more heavily on curvature. Even though the additional turning point in S-figures should degrade their detection compared to circles (Pettet, 1999), contour integration should improve more strongly with decreasing curvature because antagonistic influences of diminishing closure are absent. It is important to note that the closure-effect was not measured by directly comparing circles and S-figures. The closure-effect is defined as a shallower increase or even a decrease in performance with decreasing curvature and concomitant increasing gap size in circles compared to S-figures, i.e., a figure $\times$ gap/curvature interaction.

2. Methods

All stimuli were presented on a 19′ raster monitor (Sync Master 1100DF) controlled by a PC with a spatial resolution of 1280×1024 pixels and a refresh rate of 72 Hz. Participants were instructed to fixate a central red dot during all experiments. Viewing distance was 65 cm, resulting in a display size of $31.8 \times 25.7°$ of visual angle. All contours were constructed from and embedded in a distracting surround of Gabor elements (see Fig. 1).

2.1. Placing of the contour and distracter elements

The Gabor elements were defined as the product of a circular Gaussian with an oriented sinusoid as described by:

$$\left(\sin\left(\frac{2\pi x}{\lambda_x}\right) - \delta I\right)\frac{1}{\sigma^2 2\pi}\exp\left(\frac{-x^2 - y^2}{2\sigma^2}\right)$$

The Gabor elements were subsequently rotated to change their orientation according to the stimulus constraints described below. The spatial frequency of the Gabor elements was 2 c/deg i.e. $\lambda = 2\sigma$. The diameter of the Gabor elements of 0.5° corresponded to two standard deviations $\pm$ 1 SD; $\sigma = 0.25°$ of the circular Gaussian.[1]

To construct the contours, the centre of each Gabor element belonging to a contour was initially placed on an imaginary line with the shape of the contour. The centres of all contour elements were placed on these imaginary lines at a distance of 1.7° from all adjacent contour elements. Subsequently, each contour element was moved along these imaginary lines while the possible motion amplitude was restricted to a normal distribution with sigma = 0.25°. All contour elements had to retain a minimum distance of 0.5° from all adjacent contour elements; otherwise the whole contour was replaced. Mean contour-to-contour element distance remained at 1.7°. As described in detail below, for the first trial of each experimental run the orientations of all contour elements were set tangential to the imaginary line defining the contour but for subsequent trials the orientations of all contour elements usually differed from the optimally aligned arrangement.

The "centre of gravity" for an entire contour, which was defined as the arithmetic mean of the coordinates of all contour elements, was always placed between 5.5° and 6.5° eccentricity. This restriction of placing the contours within the display served to control for the variability in contour location between contour types as well as to avoid major performance variance due to variable eccentricity (Hess & Dakin, 1997, 1999; Nugent, Keswani, Woods, & Peli, 2003). This placement further allowed to present all contours used in this study entirely on one side of the display. During the presentation the contours appeared pseudo-randomly on the left or right side of the display.

The routine to achieve comparable element density characteristics for contour and distracter elements was adopted from Field et al. (1993) and Braun (1999) and is described in more detail in earlier studies (Mathes & Fahle, 2007; Mathes, Trenner, & Fahle, 2006). In short, the display was divided into squares, each containing a randomly oriented distracter element. To achieve a balanced distribution between contour and background elements each distracter element could change its position while keeping the mean element-to-element constant for both contour and distracter elements. Tests confirmed that the mean distance of 1.7° between nearest "natural" neighbours as assigned by the Delaunay triangulation (Barber, Dobkin, & Huhdanpaa, 1996) was achieved for both contour and distracter elements.

Eliminating the possibility to integrate the contours by using orientation cues (either by randomising the orientations of all Gabor elements or by presenting circular instead of oriented Gabor elements) yielded performance at chance level in trained subjects for both open and closed contour types ($N = 14$). Contour detection therefore results exclusively from spatially integrating single elements to a contour based on orientation cues, rather than on position cues.

2.2. General principles for constructing the contour types

For experiments 1 and 2 all contour types used can be described as variations of the closed circle. This closed circle varied in three aspects: number of contour elements, curvature and smoothness.

[1] We implemented the δI-value to compensate for the logarithmic luminance transfer function of the visual system, i.e., following Weber's law the arithmetic mean of a Gabor stimulus not necessarily equals its perceived mean luminance as tested with a homogeneous field. To equalize the perceived mean luminance of the Gabor elements with the background luminance, i.e., to achieve that the display appears as homogenously grey when viewed from a distance, the value of the balancing constant $\delta I = -0.19$ was experimentally determined by BM and DT (see Acknowledgements). This resulted in a Michelson contrast of 0.9 and a mean luminance of the Gabor elements of approximately 6 cd/m^2 less than the background luminance which was 51.2 cd/m^2. The Michelson contrast was calculated from the actually presented minimum and maximum luminance of the Gabors.

2.2.1. Number of contour elements

In experiment 1 all contour types were presented either with 7, 8 or 9 elements (see Fig. 1B). In experiment 2 we additionally measured performance for contours of 12 elements.

2.2.2. Gap size/curvature

In contour integration the contours are composed of a discontinuous string of oriented elements, i.e., the difference between open and closed contours is more accurately described as an additional gap for open contours which is clearly larger than the "regular" gap (in polar angle) between all other adjacent contour elements. Furthermore, the regular gap size depends on the angle between the positions of neighbouring elements of the contour, i.e., the curvature of the contour. For closed contours the curvature increased with decreasing numbers of contour elements. The mean curvature for the closed circle was 51° for the 7, 45° for the 8, 40° for the 9, and 30° for the 12 element contour. To compensate for the resulting differences of the regular gap size with increasing number of contour elements, we increased the size of the regular gap for the closed circle to construct open contour types. The regular gap of the closed circle therefore served as the baseline and we tested performance differences caused by increasing this baseline gap size. In experiment 1 the increased gap was either 22.5° or 45° in polar angle larger than the baseline gap between contour elements of the closed contour (see Fig. 1A). In experiment 2 we also tested a gap size of 180°.

For each length the closed circle always has the highest curvature and the introduction of a gap always leads to a concomitant reduction of the contour's curvature. This reduction was of a comparable ratio for all contour lengths (curvature of open circle/curvature of closed circle ≈0.93 for the 22°, 0.86 for the 45° and 0.43 for the 180° circle for all contour lengths).

2.2.3. Smoothness

The S-figures tested were identical to the circles except for a change in contour direction at half-length. For example, the 0°-S-figure was identical to the closed circle except for the turning point at half length, i.e., the two halves of the circle were arranged one below the other and with their openings pointing in opposite directions (see Fig. 1A). Similarly, the 45°-S-figure was identical to the 45°-circle except for the turning point at half length, and so on. The mean of the absolute values of the angles between adjacent contour elements was identical to the circles, i.e., highest for the 0°-S-figures.

Each circular contour type was labelled by its gap size and the number of its elements. The same labels were used for the S-figures, i.e., the labels for the gap sizes refer to the corresponding circular contour types. In experiment 3 we used open and closed ellipses and their S-shaped counterparts (S-ellipses) with a length of either 9 or 11 elements.

2.3. Staircase procedure

Each contour type was tested in a separate run. During each run the orientations of the contour elements with respect to the imaginary contour line varied. This deviation of orientation is described by the angle α (Field et al., 1993). For $\alpha = 0°$ the orientations of the contour elements were set tangential to the imaginary line of the contour. For $\alpha > 0°$ the orientations of the contour elements differed randomly either clockwise or anti- clockwise by α degree from the optimally aligned arrangement (orientation jitter, see Fig. 1C). The test started with the aligned version of the contour and varied α following a staircase procedure (QUEST; Watson & Pelli, 1983) to define the maximally tolerable orientation jitter at threshold performance. The standard criterion of 75% correct responses was defined as the threshold. After each stimulus presentation, participants had to indicate the position of the main part of the contour (left or right) by pressing a right- or left hand button (Binary-Forced-Choice procedure). The order of the contour types tested was counterbalanced between subjects in all experiments. Each contour type was measured twice. For each run the contour type tested was displayed 80 times, each time for 500 ms. The presentation time used is comparable to other studies investigating contour integration by varying the orientation jitter α (Field et al., 1993; Mathes & Fahle, 2007; Mathes et al., 2006; Poom, 2002). However, the presentation time allowed for approximately 2–3 saccades (Antes & Penland, 1981; Zingale & Kowler, 1987).

2.4. Statistical analysis

ANOVAs (figure × gap/curvature × number of contour elements) were conducted to compare orientation jitter α (in degree) at threshold performance. For all ANOVAs the Greenhouse–Geisser corrected *p*-values are reported. For post hoc comparison curvature-depended performance was tested using planned *t*-test comparisons between closed and open circles (or ellipses). For the S-figures the corresponding *t*-tests were conducted. *p*-Values of all post hoc *t*-tests were corrected using the Bonferroni procedure.

3. Experiment 1: circles with bottom or top openings and corresponding S-figures

3.1. Subjects

Thirteen subjects (9 female) aged between 21.7 and 28.5 years (mean: 25.7, *SD*: 2.3) participated. Participants for all experiments were screened for normal or corrected-to-normal visual acuity by means of the Freiburger Visus Acuity Test (Bach, 1996).

3.2. Contour types of experiment 1

As described above, the circles consisted of either 7, 8 or 9 elements and gap size was either by 0° (closed circle), 22.5° or 45° larger than the baseline gap (see Section 2). For seven subjects the gap always pointed downwards, for the remaining six subjects the gap always pointed upwards (see Fig. 1A). The S-figures were always presented in an upright position. For the seven-subject group the S-figures always resembled an S, while for the other subjects the S-figures resembled a question mark, i.e., two mirror symmetric versions of (open and closed) circles and S-figures were created to control for possible direction-specific effects. This procedure ensured comparable variation in the shape of the contours for closed circles (which could only have one shape), open circles and S-figures (which were now restricted to one shape, too; Tversky et al., 2004).

3.3. Results and discussion of experiment 1

The maximally tolerated orientation jitter α at threshold was significantly larger, i.e., performance was better for circles than for S-figures ($F(1,12) = 127.0$, $p < .001$). The impact of curvature on detection is opposite in circles versus S-figures as indicated by a significant figure × gap/curvature interaction ($F(2,24) = 3.8$, $p < .05$, see Fig. 2—top left).

Furthermore, performance increased with increasing contour length from 7 to 8 and also from 8 to 9 contour elements ($F(2,24) = 67.3$, $p < .001$; $p < .05$ for both post hoc comparisons). The improvement of performance with increasing number of contour elements was stronger for S-figures as indicated by a significant figure × number of

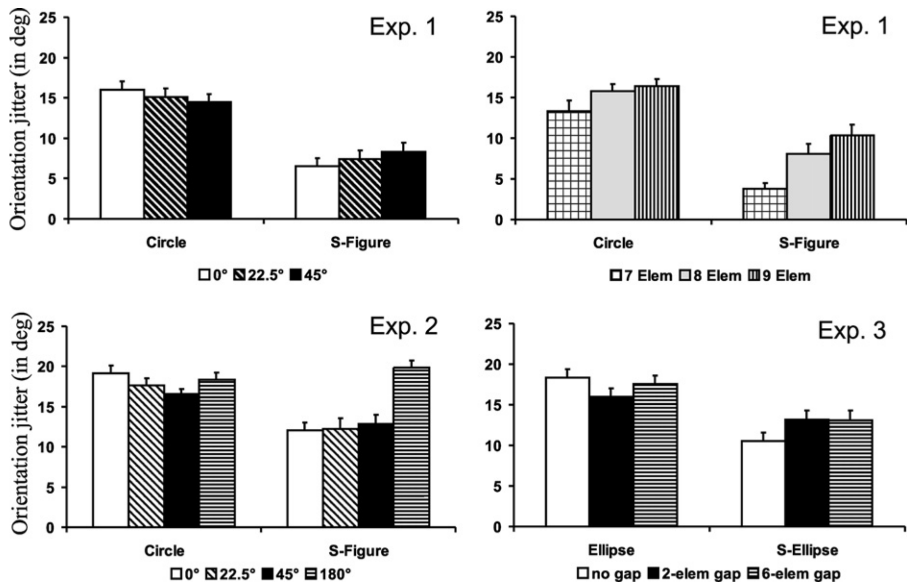

Fig. 2. Depicts the maximally tolerable orientation jitter α at threshold performance (75% of correct responses). The right side of each graph shows results for circles or ellipses, the left side for their corresponding S-figures. Error bars indicate standard errors. **Top left**: Depiction of the interaction of figure × gap/curvature in experiment 1. The results are shown separately for the closed circles (white) and open circles with a gap size of 22.5° (diagonal stripes) and of 45° (black) and their corresponding S-figures. Similar to the bottom row, black indicates the gap size eliciting the maximal closure-effect. **Top right**: Depiction of the interaction of figure × number of contour elements in experiment 1. The results are shown separately for contours of 7 (chequered), 8 (grey) and 9 elements (vertical stripes). **Bottom left**: Results of experiment 2 for the closed circles (white) or open circles with a gap size of 22.5° (diagonal stripes), of 45° (black) and of 180° (parallel stripes) and corresponding S-figures. **Bottom right**: Results of experiment 3 for the closed ellipses (white) or open ellipses with a gap size of 2 (black) or 6 missing elements (parallel stripes) The number of visible elements was identical between open and closed ellipses and their corresponding S-ellipses (see text for further details).

contour elements interaction ($F(2,24) = 3.6$, $p < .05$, see Fig. 2—top right).

These results confirm that contour saliency increases with increasing number of contour elements (Braun, 1999; Li & Gilbert, 2002) and decreases with the presence of a turning point (Pettet, 1999). The impact of curvature on detection is opposite in circles and S-figures suggesting differences in the underlying neuronal mechanisms. As expected the improvement of performance with decreasing curvature was indeed stronger for S-figures than for circles in experiment 1. Closed circles tended be better visible than open circles despite their higher curvatures.

4. Experiment 2: circles with right or left side openings and corresponding S-figures

In experiment 2 we presented the open circles with their openings to the right or left side. This allowed to measure whether the effect of closure is different for larger gap sizes, because with the opening presented to the right or left side we could present contours with larger gap sizes than used in experiment 1 entirely on one side of the display. Similarly, presenting the openings to the right or left hand side gave us the possibility to add to the experimental design contours consisting of more elements. The centres of the contours were still placed between 5.5° and 6.5° eccentricity.

4.1. Subjects

Eight subjects (6 female) aged between 22.0 and 28.2 years (mean: 24.3, *SD*: 2.1) participated.

4.2. Contour types of experiment 2

The circles consisted of either 7, 8, 9 or 12 elements and gap size was larger by either 0° (closed circle), 22.5°, 45° or 180° than the baseline gap. For four subjects the gap always pointed to the right, for the remaining four subjects the gap always pointed to the left (see Fig. 3A). The S-figures were presented as in experiment 1.

4.3. Results and discussion of experiment 2

As in experiment 1, the maximally tolerable orientation jitter α increased significantly for circles compared to S-figures ($F(1,7) = 28.4$, $p < .01$) and similarly for long compared to short contours ($F(3,21) = 99.7$, $p < .001$). Performance increased more with increasing number of contour elements for S-figures as indicated by a significant figure × number of contour elements interaction ($F(3,21) = 10.8$, $p < .01$). Post hoc comparisons confirmed that performance increased from 7 to 8 and also from 9 to 12 elements ($p < .01$ for both comparisons). Moreover, performance improved with decreasing curvature as indicated by a significant effect for gap/curvature ($F(3,21) = 53.3$,

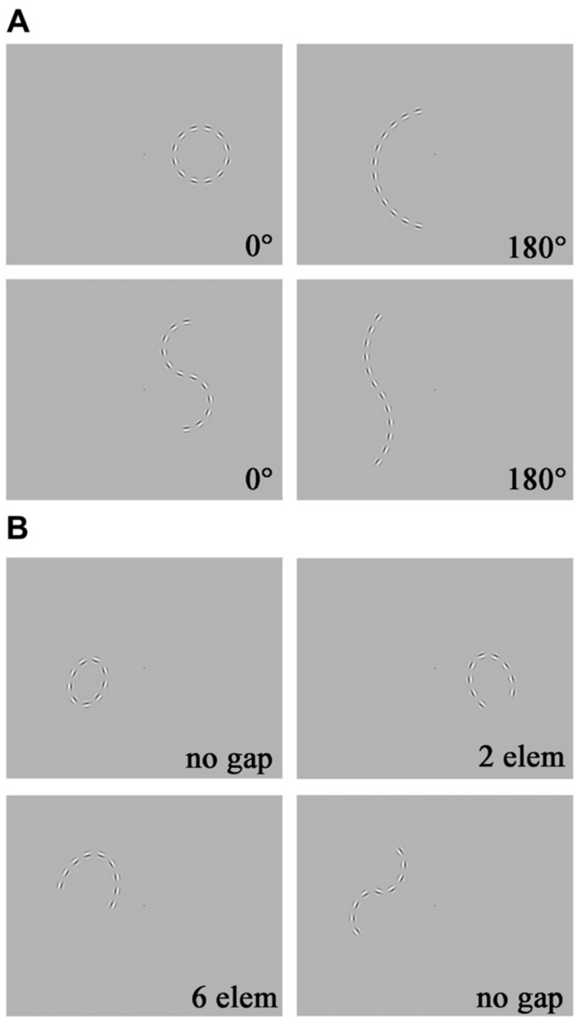

Fig. 3. (A) Extending the experimental design of experiment 1, open circles with a gap size of 180° and their corresponding S-figures were tested during experiment 2. In experiment 2 the gaps always pointed to the side. During the experiments the contours were embedded in a surround of pseudo-randomly oriented distracters. (B) Illustrates the stimuli used in experiment 3. The mean curvature of the ellipses decreased with increasing gap size. The S-ellipses were created by introducing a turning point at the midpoints. Stimuli occurring on the right were mirror-symmetric to stimuli occurring on the left hand side of the display. The gaps always pointed outwards.

$p < .001$). Most importantly the main effect of gap/curvature for the circles was only supported by the 180°-circle as indicated by a significant figure × gap/curvature interaction ($F(3,21) = 19.5$, $p < .001$, see Fig. 2—bottom left). Post hoc comparisons further demonstrate that performance for the 0°-S-figure is worse than for the 180°-S-figure ($p < .01$). This was not the case for the circle. The three-way interaction between figure × gap/curvature × number of contour elements ($F(9,63) = 6.6$, $p < .01$) possibly indicates that the closure effect decreased with increasing number of contour elements.

Experiment 2 replicates the findings of experiment 1. Closure reverses the effect of increasing detection performance with decreasing curvature. However, closure has no effect for very low curvatures, i.e., circles with large gaps (180°-circle). This result indicates that closure does not enhance contour saliency beyond the performance level for very low curvatures.

4.3.1. Combining the results of experiments 1 and 2

In order to compare the results of experiments 1 and 2 and to increase the power of analysis we combined the data sets of both experiments and re-analysed the main effect for gap/curvature and the interaction between figure × gap/curvature. For experiment 2, only those task conditions which mirrored experiment 1 were used, i.e., all runs with a contour length of 12 elements as well as the 180°-circles and 180°-S-figures of all lengths were excluded. There was no main effect for curvature, but a significant interaction between figure × gap/curvature ($F(2,38) = 5.9$, $p < .01$). The orientation jitter α for the closed circle was higher than for the 45°-circle ($p < .05$ for post hoc comparison). This was not the case for the S-figures. This result confirms that the impact of curvature was opposite for circles and S-figures. Fig. 4 demonstrates that this trend occurs regardless of the number of elements defining the contour. For the contours consisting of 7, 8 or 9 elements the combined results for experiments 1 and 2 are displayed. The contour length of 12 elements was only measured during experiment 2, i.e., only the results of these 8 subjects are reflected in Fig. 4.

The combined analysis of experiments 1 and 2 demonstrated that closure affects all directions of the gap (up, down, left or right). Although we have not measured enough gap sizes to exactly determine the maximum, our results demonstrate that contour salience for the circles used in this study is minimal for the 45° gap. In visual search experiments where open targets are embedded between closed distracters (Mori, 1997; Treisman & Souther, 1985) or concave-shaped targets are embedded between barrel-shaped distracters (Elder & Zucker, 1993, 1994) closure is regarded to be a continuous stimulus feature which gradually degrades with increasing gap size (Elder & Zucker, 1993, 1994; Mori, 1997; Treisman & Souther, 1985). Although contour integration paradigms differ from visual search paradigms it might be tentatively assumed that the 22.5° circle still profits from partial perceptual closure leading to performance levels similar to the 0° circle.

5. Experiment 3: ellipses with outward openings and corresponding S-shaped figures

In experiments 1 and 2 the centres of the contours were placed at identical eccentricities for all contours. In experiment 2, however, the openings were directed towards the fixation point in half of the trials, for example when the circle was open to the right and displayed on the left side of the display (see Fig. 3A). In these instances contour integration might be more difficult for open than for closed contours, because the gap occurs at the critical position where the distance between the contour and the fixation point is always the smallest for the closed contour. This

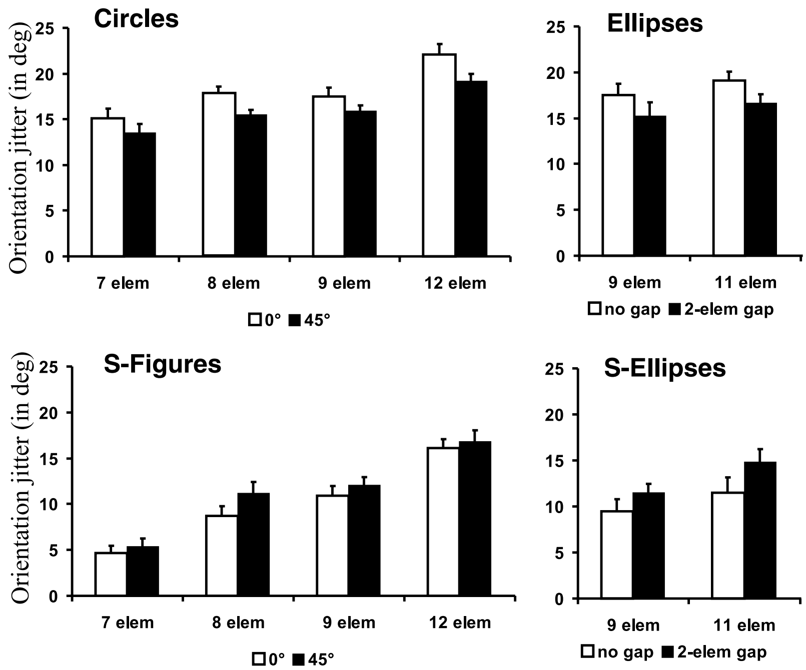

Fig. 4. Depicts the maximally tolerable orientation jitter α at threshold (75% of correct responses). Results are shown separately as a function of the number of contour elements used. Error bars indicate standard errors. The impact of curvature was different for circles and ellipses than for the corresponding S-figures. **Top left**: Results are shown separately for the closed circles (white) and the open 45°-circles (black). For the contours consisting of 7, 8 or 9 elements the combined results for experiments 1 and 2 are displayed ($n = 21$). The contour length of 12 elements was only measured during experiment 2, i.e., only the results of the 8 subjects of experiment 2 are displayed. **Bottom left**: The corresponding results for the 0°-S-figure (white) and 45°-S-figure (black). **Top right**: Results for the closed ellipses (white) and the open ellipses with a gap of 2 elements (black) as measured during experiment 3, $n = 8$. **Bottom right**: The corresponding results for the S-ellipses.

asymmetry therefore possibly leads to an overestimation of the effect of closure. Although this phenomenon did not occur in experiment 1, we run an extra control experiment, since contour integration seems to depend on eccentricity (Hess & Dakin, 1997, 1999; Nugent et al., 2003).

In experiment 3 the gaps were always pointing outwards. This lead to shape uncertainty, because the shape of the figures presented on the right versus left side of the display would differ. To ensure comparable figure uncertainty for all contour types we used ellipses instead of circles in experiment 3. Ellipses, contrary to closed circles, can be tilted and therefore vary in their appearance similarly to the open contours. As in experiment 2, we used small and large gaps to test whether, with increasing gap size, performance drops first and recovers later when the gap becomes relatively big.

5.1. Subjects

Eight subjects (5 female) aged between 23.9 and 32.8 years (mean: 27.1, *SD*: 2.9) participated.

5.2. Contour types of experiment 3

The ellipses and their S-shaped counterparts (S-ellipses) consisted of 9 or else 11 elements. The centres of the contours were placed as in experiments 1 and 2 between 5.5° and 6.5° eccentricity. The major axes of the contours were tilted mirror-symmetrically for contours appearing on the right or left hand side of the display (see Fig. 3B). The ratio between the main and the minor axis of an ellipse can be described by a parameter e which varies between 0 and 1 ($e = 0$ corresponds to a circle, $e = 1$ corresponds to a line). We used ellipses with $e = 0.7$ throughout the experiment. Except for the circles (as special cases of an ellipse), the element-to-element curvature differs along the elliptical contour. However, it is the mean curvature of a contour that seems to determine detection performance (Pettet, 1999). The curvature is maximal at the vertices of the ellipse. To reduce the mean curvature of the ellipses by incorporating gaps we constructed larger ellipses and then excluded the elements around the lower vertex which pointed outwards (see Fig. 3B). For example, we constructed ellipses with 9, 11 and 15 elements and excluded 0, 2 or 6 elements to achieve contours with the same number of contour elements (9 elements) but different gap sizes. The gap always pointed outwards, i.e., the gap occurred on the right if the stimulus appeared on the right while the gap occurred on the left when the stimulus appeared on the left side of the display (see Fig. 3B). The S-ellipses were identical to the ellipses except for a change in contour direction at the upper vertex of the ellipse, i.e., at half-length.

5.3. Results and discussion of experiment 3

Performance for the ellipses was better than for the contours including a turning point (S-ellipses, $F(1,7) = 70.9$,

$p < .001$). The impact of curvature was different between ellipses and S-ellipses as indicated by a significant figure × gap/curvature interaction ($F(2,14) = 8.2$, $p < .01$), see Fig. 2—bottom left and Fig. 4—right. Performance for the closed ellipses was better for the open ellipse with the smaller gap ($p < .05$). This was, however, not the case for the S-ellipses. The improvement of performance with increasing number of contour elements remained a trend ($p = .052$).

Experiment 3 confirms the results of experiments 1 and 2 and ensures that the effect of closure also occurs when the minimum distance between the fixation point and the nearest contour element was not smaller in open than in closed contours. Experiment 3 demonstrates that the effect of closure occurs also when element-to-element curvature differs along the contour.

6. General discussion

We investigated the impact of closure on contour integration. The facilitation of contour integration by closure yields different patterns of results for circles compared with S-figures. Performance for circles decreased with increasing gap size, even though increasing gap size leads to a concomitant decrease in curvature. Performance decreased in circles up to a gap size of 45°, indicating that closure might—to a certain extend—compensate for the low detectability of highly curved contours. For a 180° gap performance was comparable to the closed circle (0° gap). Hence, performance mirrored the loss of the beneficial influence of closure with increasing gap size, except for the 180° gap. On the other hand, performance for S-figures increased monotonically with decreasing curvature. As all S-figures were open, performance for the S-figures relied on curvature only. Similar results were found for ellipses.

Recent studies challenged the concept that better performance for closed compared to open contours results from closure. It was assumed that the greater salience of closed compared to open contours had been overestimated due to additional advantages for the closed contour compared to the open contours (Braun, 1999; Pettet, 1999; Pettet et al., 1998; Tversky et al., 2004). In this study, we systematically compared contour detection for closed contours with that for open contours even when open contours do not include additional turning points or fewer elements than closed ones. Our results demonstrate that the facilitating influence of closure on contour integration can be observed in most subjects (see Fig. 5), supporting the concept that closure has a positive influence on grouping and perception of objects.

However, our results also demonstrate that of all properties of the contours varied in this study (closure, curvature, smoothness (i.e., the occurrence or absence of turning points), and number of contour elements), closure did not elicit the largest modulations of performance. The introduction of a turning point, i.e., producing the S-figures, lead to a tremendous drop in performance. This finding, therefore, supports the notion that contour integration relies heavily on smoothness of a contour (Kovacs & Julesz, 1993; Pettet, 1999; Pettet et al., 1998) and indicates the importance of both smoothness and closure on contour integration. Furthermore, our results support the earlier finding that visibility of contours near detection threshold improves by increasing the number of contour elements (Braun, 1999; Li & Gilbert, 2002).

The relatively small increase in performance for closed compared to open, circular contours may result from the paradigm used. In this study, we compared contour integration for closed contours with that for open, less curved contours. Performance regularly increases with decreasing curvature in contour integration experiments (e.g., Field et al., 1993). Hence, open contours should be easier detected than closed, more curved ones and this effect might have diminished the positive effect of closure. And indeed, in our study contour detection was similar for closed contours and open contours with the largest gap size, i.e., lowest curvature, tested. Performance for straight or nearly straight contours might be even better (Pettet, 1999). Our results therefore suggest that although closure might compensate for the low detectability of highly curved contours, closure does not enhance contour saliency beyond those performance levels obtained by highly salient and open contours, such as long and straight lines.

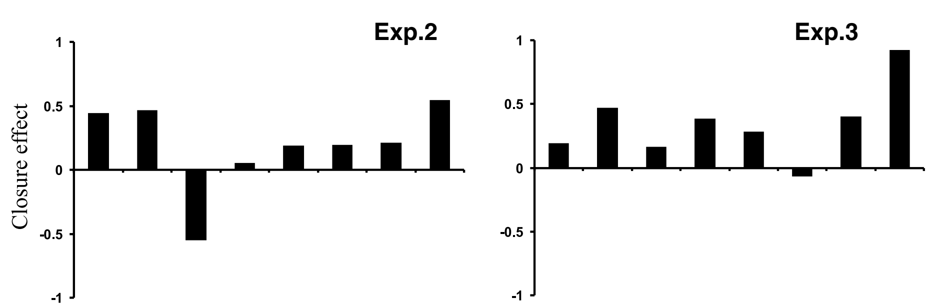

Fig. 5. Strength of the maximum closure effect of experiments 2 and 3 in all individual subjects. In Fig. 2 the task condition showing the maximal closure effect was always depicted in black. For this graphs, the ratio of the closed contour compared to task condition showing the maximum closure effect was subtracted from the corresponding ratio for the S-figures. Positive values indicate a pattern of performance supporting the beneficial influence of closure on contour integration.

Furthermore, measuring orientation jitter may not be the optimal measure for the closure effect as not all studies varying orientation jitter reported better performance for closed compared to open contours (Tversky et al., 2004). Additionally, because of the element-to-element distance of 1.7° used in our study contour integration might have been more difficult compared to other studies using smaller element-to-element distances. In general, contour integration studies investigating contour closure vary in many respects, such as presentation time (which might or might not allow for eye-movements), element-to-element distance and the measure used to quantify performance (see Section 1). Furthermore, some studies on contour integration utilise line elements and other studies use oriented Gabor elements and processing of oriented line and Gabor elements might not be absolutely equal (Westheimer, 1998). Finally, the closure effect might also be larger when all Gabor elements used are of the same phase (as in our study) than when the phase of the Gabor elements is varied (Braun, 1999). It might be interesting for future studies to asses how the closure effect depends on these variables.

Functional imaging studies indicate that information about both the contour and its surround is processed to achieve contour integration in a network involving various visual areas (Altmann, Bülthoff, & Kourtzi, 2003; Altmann, Deubelius, & Kourtzi, 2004; Kourtzi, Tolias, Altmann, Augath, & Logothetis, 2003). More specifically, early visual areas seem to process local orientation information of the contour elements while higher visual areas, such as the lateral occipital complex, process the global shape of the contour (Dumoulin & Hess, 2006; Kourtzi & Huberle, 2005; Kourtzi & Kanwisher, 2001). Facilitation of contour integration by closure may occur on both processing stages.

Neural simulation studies have investigated the involvement of local interactions between contour elements in the closure-effect (Pettet et al., 1998; Tversky et al., 2004). They conjecture that the closure-effect derives from a facilitation between nearby and similarly oriented elements which propagates multiple times around the closed contour, producing reverberating activity and enhancing contour detection (Pettet et al., 1998). However, if facilitation spreads in both directions from a single oriented edge element, then even two elements in a contour will produce some reverberating activity by mutual facilitation between these two contour elements. It follows that a forward-backward reverberation in an open contour will "assimilate" to circular reverberation in a closed contour with increasing contour length. And indeed, the closure-effect in long contours is relatively small (Braun, 1999).

On the other hand, mathematically well-defined probabilistic theories of contour integration have put forward the notion of a strictly directed process of both, contour generation and contour integration (Williams & Thornber, 2001). Here, strictly directed means that after an element has facilitated its right hand neighbour facilitation can only propagate further in the same direction, but not immediately back to the element where facilitation originated. Experimental data revealed that such uni-directional association fields may come closer in explaining contour integration processes in the brain than models using bi-directional association fields (e.g., Schinkel, Pawelzik, & Ernst, 2006). Although this has not yet been tested, it might be assumed that such a directed process of contour integration should in many situations also produce a clear difference in saliency between closed and open contours since reverberating activity would occur only in closed contours.

Additionally, the facilitation of contour integration by closure might rely on higher level visual processing, because identification of fragmented objects by perceptual closure relies heavily on the activation of the lateral occipital complex (Doniger et al., 2000; Sehatpour, Molholm, Javitt, & Foxe, 2006). Furthermore, in visual search paradigms closure seems not to be processed pre-attentively (Treisman & Souther, 1985). In this view does contour integration depend on both lower and higher visual processing, and the influence of closure on contour integration is described as a modulation of higher level processing, possibly by increasing the efficiency of the object signals. In accordance, electrophysiological results demonstrate that salient contours are processed within 150 ms but that processing time increases for higher task demands, for example by introducing gaps and turning points into the contours (Mathes et al., 2006). To achieve a comparable timing in the electrophysiological response the orientation jitter for closed contours can be enhanced compared to open contours, again indicating more efficient processing for closed contours when the orientation jitter is similar between open and closed contour types (Mathes & Fahle, 2007).

In conclusion, we found that closure facilitates contour integration in smooth contours. Compared to closed contours, performance is lower for open, circular contours with small gap sizes. Performance is comparable between closed contours and contours of the largest gap size tested. This indicates that at the highest levels of contour integration performance might rely on contour properties other than closure. Closure facilitates contour integration for contours sufficiently near detection threshold.

Acknowledgments

Supported by the Deutsche Forschungsgesellschaft (German Research Foundation; SFB517/C10). We thank D. Trenner for invaluable support by generating the computer code, C. Schütze for helpful discussions about the experimental design as well as M. Limberg and M. Harms for help with performing some of the experiments and data input. We also thank Dr. U. Ernst and N. Schinkel for helpful discussions regarding the computer code and contour integration models as well as for their comments on drafts of this manuscript.

References

Altmann, C. F., Bülthoff, H. H., & Kourtzi, Z. (2003). Perceptual organization of local elements into global shapes in the human visual cortex. *Current Biology, 13*, 342–349.

Altmann, C. F., Deubelius, A., & Kourtzi, Z. (2004). Shape saliency modulates contextual processing in the human lateral occipital complex. *Journal of Cognitive Neuroscience, 16*, 794–804.

Antes, J. R., & Penland, J. G. (1981). Picture context effects on eye movement patterns. In D. F. Fisher, R. A. Monty, & J. W. Senders (Eds.), *Eye movements: Cognition and visual perception* (pp. 157–170). New Jersey: Lawrence Erlbaum Associates.

Bach, M. (1996). The "Freiburg Visual Acuity Test"—Automatic measurement of visual acuity. *Optometry and Vision Science, 73*, 49–53.

Barber, C. B., Dobkin, D. P., & Huhdanpaa, H. (1996). The quickhull algorithm for convex hulls. *ACM Transactions on Mathematical Software, 22*, 469–483.

Beaudot, W. H., & Mullen, K. T. (2003). How long range is contour integration in human color visual? *Vision Neuroscience, 20*, 51–64.

Braun, J. (1999). On the detection of salient contours. *Spatial Vision, 12*, 211–225.

Doniger, G. M., Foxe, J. J., Murray, M. M., Higgins, B. A., Snodgrass, J. G., Schroeder, C. E., et al. (2000). Activation timecourse of ventral visual stream object-recognition areas: High density electrical mapping of perceptual closure processes. *Journal of Cognitive Neuroscience, 12*, 615–621.

Dumoulin, S. O., & Hess, R. F. (2006). Modulation of V1 activity by shape: Image-statistics or shape-based perception? *Journal of Neurophysiology, 95*, 3654–3664.

Elder, J., & Zucker, S. (1993). The effect of contour closure on the rapid discrimination of two-dimensional shapes. *Vision Research, 33*, 981–991.

Elder, J., & Zucker, S. (1994). A measure of closure. *Vision Research, 34*, 3361–3369.

Field, D. J., Hayes, A., & Hess, R. F. (1993). Contour integration by the human visual system: Evidence for a local association field. *Vision Research, 33*, 173–193.

Hess, R., & Field, D. (1999). Integration of contours: New insights. *Trends in Cognitive Sciences, 3*, 480–486.

Hess, R. F., & Dakin, S. C. (1997). Absence of contour linking in peripheral vision. *Nature, 390*, 602–604.

Hess, R. F., & Dakin, S. C. (1999). Contour integration in the peripheral field. *Vision Research, 39*, 947–959.

Kourtzi, Z., & Huberle, E. (2005). Spatiotemporal characteristics of form analysis in the human visual cortex revealed by rapid event-related fMRI adaptation. *Neuroimage, 28*, 440–452.

Kourtzi, Z., & Kanwisher, N. (2001). Representation of perceived object shape by the human lateral occipital complex. *Science, 293*, 1506–1509.

Kourtzi, Z., Tolias, A. S., Altmann, C. F., Augath, M., & Logothetis, N. K. (2003). Integration of local features into global shapes: Monkey and human FMRI studies. *Neuron, 37*, 333–346.

Kovacs, I., & Julesz, B. (1993). A closed curve is much more than an incomplete one: Effect of closure in figure-ground segmentation. *Proceedings of the National Academy of Sciences of The United States of America, 90*, 7495–7497.

Li, W., & Gilbert, C. D. (2002). Global contour saliency and local colinear interactions. *Journal of Neurophysiology, 88*, 2846–2856.

Mathes, B. & Fahle, M. (2007). The electrophysiological correlate of contour integration is similar for colour and luminance mechanisms. *Psychophysiology*, in press.

Mathes, B., Trenner, D., & Fahle, M. (2006). The electrophysiological correlate of contour integration is modulated by task demands. *Brain Research, 1114*, 98–112.

Mori, S. (1997). Effect of absolute and relative gap sizes in visual search for closure. *Canadian Journal of Experimental Psychology, 51*, 112–125.

Nugent, A. K., Keswani, R. N., Woods, R. L., & Peli, E. (2003). Contour integration in peripheral vision reduces gradually with eccentricity. *Vision Research, 43*, 2427–2437.

Pettet, M. W. (1999). Shape and contour detection. *Vision Research, 39*, 551–557.

Pettet, M. W., McKee, S. P., & Grzywacz, N. M. (1998). Constraints on long range interactions mediating contour detection. *Vision Research, 38*, 865–879.

Poom, L. (2002). Visual binding of luminance, motion and disparity edges. *Vision Research, 42*, 2577–2591.

Schinkel, N., Pawelzik, K. R., & Ernst, U. A. (2006). Robust integration and detection of noisy contours in a probabilistic neural model. *Neurocomputing*, 211–217.

Sehatpour, P., Molholm, S., Javitt, D. C., & Foxe, J. J. (2006). Spatiotemporal dynamics of human object recognition processing: An integrated high-density electrical mapping and functional imaging study of "closure" processes. *Neuroimage, 29*, 605–618.

Treisman, A., & Souther, J. (1985). Search asymmetry: A diagnostic for preattentive processing of separable features. *Journal of Experimental Psychology–General, 114*, 285–310.

Tversky, T., Geisler, W. S., & Perry, J. S. (2004). Contour grouping: Closure effects are explained by good continuation and proximity. *Vision Research, 44*, 2769–2777.

Watson, A. B., & Pelli, D. G. (1983). QUEST: A Bayesian adaptive psychometric method. *Perception & Psychophysics, 33*, 113–120.

Wertheimer, M. (1923). Untersuchungen zur Lehre von der Gestalt. *Psychologische Forschung, 4*, 301–350.

Westheimer, G. (1998). Lines and Gabor functions compared as spatial visual stimuli. *Vision Research, 38*, 487–491.

Westheimer, G. (1999). Gestalt theory reconfigured: Max Wertheimer's anticipation of recent developments in visual neuroscience. *Perception, 28*, 5–15.

Williams, L. R., & Thornber, K. K. (2001). Orientation, scale, and discontinuity as emergent properties of illusory contour shape. *Neural Computation, 13*, 1683–1711.

Zingale, C. M., & Kowler, E. (1987). Planning sequences of saccades. *Vision Research, 27*, 1327–1341.